

Dynamic Ordering and Transverse Depinning of a Driven Elastic String in a Disordered Media

C. Reichhardt⁽¹⁾ and C. J. Olson⁽²⁾

⁽¹⁾ *CNLS and Applied Theoretical and Computational Physics Division,*

⁽²⁾ *Theoretical and Applied Physics Divisions,*

Los Alamos National Laboratory, Los Alamos, NM 87545

(October 27, 2018)

We examine the dynamics of an elastic string interacting with quenched disorder driven perpendicular and parallel to the string. We show that the string is the most disordered at the depinning transition but with increasing drive partial ordering is regained. For low drives the noise power is high and we observe a $1/f^2$ noise signature crossing over to a white noise character with low power at higher drives. For the parallel driven moving string there is a finite transverse critical depinning force with the depinning transition occurring by the formation of running kinks.

PACS: 64.60.Ak, 71.45.Lr, 74.60.Ge

The dynamics of driven elastic media interacting with quenched disorder occurs in a wide variety of physical systems which include magnetic domain wall motion [1], nonequilibrium growth [2], models of friction [3], vortex lattice motion in superconductors [4], and charge density waves [5]. Recently an intense interest in driven elastic media with quenched disorder has been directed at *dynamical ordering* where at low applied drives the system is in a highly disordered pinned state and at a critical drive a depinning into a highly disordered moving state occurs, while at high drives the effect of the disorder is reduced and the system can regain a considerable amount of order. Particular systems where this reordering behavior has been studied extensively experimentally [6–9], theoretically [10–13], and numerically [10,14–17] include vortices in superconductors as well as charge-density wave (CDW) systems.

In the vortex system if there is no quenched disorder the vortices form an ordered crystalline state; however, in most samples there are defects which attract and pin vortices, disordering the vortex lattice. When a driving force is applied, the initial depinning transition can be plastic, with certain regions of mobile vortices tearing past pinned regions and a large number of defects generated so that the system has only a liquid like structure. For higher drives the vortices regain order; however, the pinning can still affect the structure so the vortices can have a partial anisotropic ordering or smectic structure [12]. An open question is whether the reordering transition is a true transition or a crossover.

An interesting feature of the reordered moving state is that a *transverse depinning threshold* can exist as originally proposed in Ref. [11]. Here, although the lattice is moving in the longitudinal direction, the effect of the pinning is still present in the transverse direction so that a finite transverse drive must be applied before the lattice will move in the transverse direction. Simulations [14,17] and experiments [9] on vortex lattices as well as simulations for friction models [3] have found evidence for a finite transverse depinning threshold for the longitudinal

moving systems. Other theoretical work contends that at finite T no true critical transverse depinning threshold exists; instead, due to the high pinning barriers, a pronounced *crossover* in the transverse IV curves may appear [12]. In the CDW context the effect of the quasi-particle current flowing *perpendicular* to the CDW $2k_F$ ordering wavevector was also studied theoretically [18] and in experiment [19]. An intriguing question is whether the reordering transitions and the transverse barrier seen in the vortex system occur in other types of driven elastic media, such as driven interfaces and polymers interacting with quenched disorder. An ideal way to model these systems in 2D is with a driven elastic string interacting with quenched disorder.

Previous numerical studies of driven elastic strings with disorder [20–23] employed drives perpendicular to the string and focused on the dynamics near the depinning threshold. In this case critical behavior is expected, and was observed in the form of broad distributions of avalanche sizes as well as scaling of the velocity near depinning, $v = (f - f_c)^\alpha$, as proposed by Fisher [24]. The roughness of the string as measured by the roughening coefficient exponent was 0.9 to 1.1 at depinning [20,22] and 0.5 at high drives [20], indicating that some ordering of the string was occurring as the drive increased.

In this work we investigate the continual evolution of the order and noise signatures in driven strings for both parallel and perpendicular drives. We also investigate the transverse depinning for the moving string. In the case of the perpendicular moving string we do not observe a transverse barrier; however, for the parallel driven string a transverse depinning threshold is observed which occurs through the formation of running kinks. For increasing longitudinal drives the transverse barrier decreases. Physical systems relevant to the perpendicular driven string include domain walls and moving interfaces, while systems similar to the parallel driven string include boundaries between sliding surfaces, polymers that are aligned with an applied drive in a random media, or a single stream of fluid flowing down a rough surface.

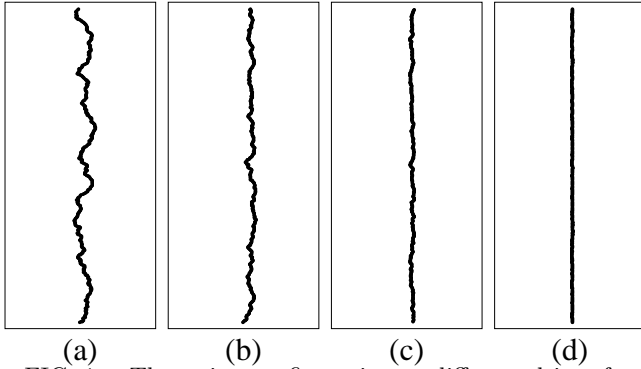


FIG. 1. The string configuration at different drives for a system with driving in the x -direction perpendicular to the string with a depinning threshold of $F_{dp} = 0.09$. (a) Right above depinning at $F_d/F_{dp} = 1.1$; (b) $F_d/F_{dp} = 1.38$; (c) $F_d/F_{dp} = 1.94$; (d) $F_d/F_{dp} = 4.4$.

We model an overdamped elastic string in $(1 + 1)$ dimensions. The string is composed of discrete particles connected by springs. The system has periodic boundary conditions in the x and y -directions and the string is connected periodically in the y -direction. The equation of motion for each particle on the string is:

$$\gamma \frac{d\mathbf{r}}{dt} = \kappa \mathbf{f}_s + \mathbf{f}_p + \mathbf{F}_d. \quad (1)$$

Here \mathbf{r} is the particle location, $\gamma = 1$ is the damping term, $\kappa = 5$ is the string elastic constant, $\mathbf{f}_s = \mathbf{r}_{i-1} - 2\mathbf{r}_i + \mathbf{r}_{i+1}$ is the spring force from the two neighboring particles, \mathbf{f}_p is the pinning force and \mathbf{F}_d is the uniform applied driving force. The pinning is modeled as attractive parabolic traps scattered randomly through the sample. The pinning force is $\mathbf{f}_p = -\sum_i^{N_p} (f_p/r_p)(\mathbf{r}_i - \mathbf{r}_k^{(p)})\Theta(r_p - |\mathbf{r}_i - \mathbf{r}_k^{(p)}|)$, where Θ is the Heaviside step function, $\mathbf{r}_k^{(p)}$ is the location of pinning site k , $f_p = 0.3$ is the maximum pinning force, and $r_p = 0.25$ is the pinning radius. The results shown here are for strings containing $N = 500$ to 2000 particles, interacting with $N_p = 4.6 \times 10^5$ pinning sites in samples of size 160×160 . We consider two types of initial conditions: one where the string is put down in its unstretched equilibrium position, and a second where the string is annealed at a finite temperature by the addition of a thermal kick. We find that when the applied drive is increased slowly enough, both methods give similar results. We apply a uniform force F_d in the x direction for perpendicular driving or the y -direction for parallel driving. We increase the driving force in increments of 0.001 and spend 30000 simulation steps at each increment, measuring the average string velocity $V_x = \sum_i^{N_i} \hat{\mathbf{x}} \cdot \mathbf{v}_i$, and $V_y = \sum_i^{N_i} \hat{\mathbf{y}} \cdot \mathbf{v}_i$. To quantify the order in the string we measure the difference ΔL in the length of the string compared to the equilibrium length, $\Delta L = \sum_i^{N_i} (|\mathbf{r}_i - \mathbf{r}_{i+1}| - r_l)$, where r_l is the equilibrium length of each string segment. We also measure the noise in the string velocity: $S(\omega) = |\int V_x(t)e^{-i2\pi\omega t} dt|^2$, and

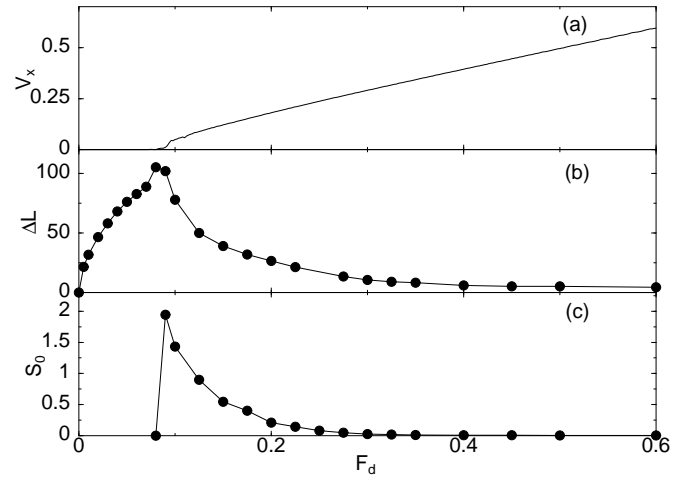


FIG. 2. (a) The string velocity V_x versus F_d for the system in Fig. 1. The string is pinned for $F_d < 0.09$. (b) ΔL versus F_d showing that the string becomes disordered as F_{dp} is approached from below, and gradually reorders for increasing $F_d > F_{dp}$. (c) Noise power S_0 versus F_d .

the noise power in one frequency octave $S_0 = \int_{\omega_2}^{\omega_1} S(\omega)$.

In Fig. 1(a-d) we show a series of snapshots of a perpendicular driven string. In Fig. 1(a) at a driving force $F_d/F_{dp} = 1.1$ very close to the depinning transition $F_{dp} = 0.09$, the string is highly disordered. Above depinning, the motion of the string is jerky, occurring in pulses or avalanches, with portions of the string immobile while other portions are moving as can be seen from the instantaneous velocity of individual beads. In Fig. 1(b) and (c) for $F_d/F_{dp} = 1.25$ and 1.75 , the string becomes less winding. Finally in Fig. 1(d), for $F_d/F_{dp} = 4.0$ the string is almost completely ordered again.

To quantify the evolution of the driven string from Fig. 1, we plot in Fig. 2(a) F_d versus $\langle V_x \rangle$ showing that the string is pinned for $F_d < 0.09$. In this case the string was initially placed in its equilibrium position. In Fig. 2(b) we plot ΔL which shows that the string is aligned for $F_d = 0$ but gradually disorders as F_{dp} is approached from below. ΔL reaches a maximum at depinning. For increasing $F_d > F_{dp}$, ΔL gradually decreases as the string orders. In Fig. 2(c) the reordering can also be seen in the noise power S_0 which is maximum at depinning and again decreases for increasing F_d . The decay of S_0 fits well to an exponential form where for $F_d > F_{dp}$, $S_0(F_d) \propto \exp(-(F_d - F_{dp}))$. We have also conducted simulations where we decrease F_d after a ramp up, and we do not observe any hysteresis in the ordering ΔL or the noise power S_0 .

In Fig. 3 we show noise spectra for the same system. Right above depinning, at $F_d/F_{dp} = 1.1$, $S(\omega)$ shows a $1/f^2$ characteristic, as seen in Fig. 3(a). For increasing drives, the string begins to move continuously and reorder. As a result, a characteristic time scale forms, the $1/f^2$ shape is lost and the higher frequencies are reduced in power, as shown in Fig. 3(b) for $F_d/F_{dp} = 4.4$. Noise

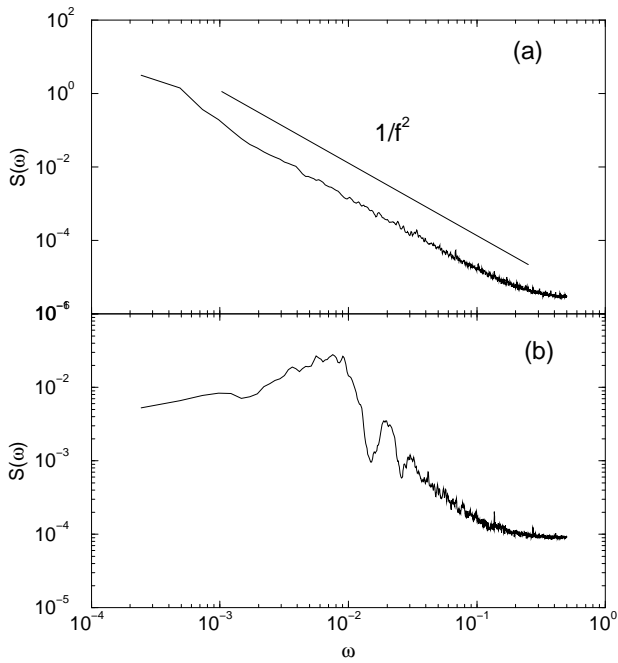


FIG. 3. (a) Noise spectra $S(\omega)$ for the system in Fig. 1 for $F_d/F_{dp} = 1.1$ showing a $1/f^2$ signal. (b) $S(\omega)$ for $F_d/F_{dp} = 4.4$ showing a characteristic time scale.

spectra for vortices have shown similar features in both experiments [25] and simulations [16]. In the vortex simulations the $1/f^2$ high noise region corresponds to the disordered plastic flow state and the low noise power region corresponds to the reordered elastic flow state.

We have repeated the same type of simulations shown in Figs. 1-3 for the parallel driven string and observe the same general features. For the parallel driven string, the depinning threshold is lower and we observe a clear washboard signal for the high drive case. We have carried out a series of simulations for varied f_p , κ , and N_p . In each case, the depinning threshold changes; however, the same general features of the reordering are observed.

To test the predictions in Ref. [11] of a critical transverse threshold for the driven string, we have conducted a series of simulations where we fix the driving force at a constant value after the string is in motion. We then slowly apply an additional driving force in the direction transverse to the initial longitudinal motion. For the perpendicular driven string the applied transverse drive is along the string and for the parallel driven string the applied transverse drive is perpendicular to the string. For the perpendicular driven string we do not observe a transverse barrier for the moving string. For a parallel driven string, in Fig. 4(a) we show the transverse driving force versus the transverse string velocity indicating that for the case of the parallel moving string there is a finite transverse pinning threshold. We note that for the moving vortex systems a finite transverse barrier occurs only when the vortices are moving in well defined channels and the transverse drive is perpendicular to these

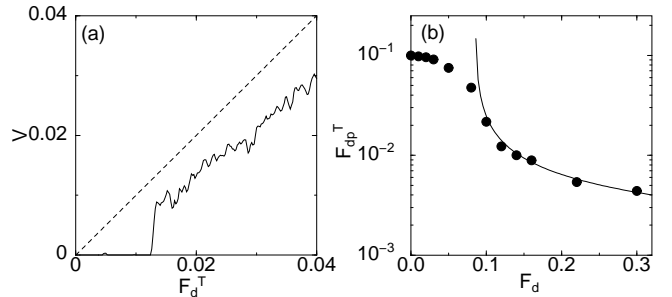


FIG. 4. (a) The transverse string velocity V versus the transverse drive F_d^T for a parallel driven string (lower curve). The parallel string drive is $F_d/F_{dp} = 1.22$. A finite transverse depinning threshold is visible. A plot of V for a system with no quenched disorder is also shown (dashed curve). (b) The transverse depinning threshold F_{dp}^T versus longitudinal drive F_d . The solid line indicates a fit to $F_{dp}^T \propto (F_d - F_{dp})^{-2/3}$

channels. The parallel moving string may be viewed as a single moving channel. In Fig. 4(b) we show that the transverse barrier decreases with increasing longitudinal velocity. In the vortex system as the longitudinal drive increases the channels straighten out and the transverse barrier decreases. In the parallel moving string the decrease in the transverse pinning threshold also corresponds to the string reordering for the higher longitudinal drives. Above the parallel depinning transition, $F_d > F_{dp}$, the data follows a power law form, $F_{dp}^T \propto (F_d - F_{dp})^{-2/3}$. In a CDW system an exponential decay would be expected [18], but for the driven string system a power law decay is predicted instead [26].

We have also investigated the dynamics of the transverse depinning for the parallel driven string, as indicated in Fig. 5, which shows a series of snapshots of the string just above the transverse depinning threshold. The transverse depinning transition is very distinct from the longitudinal depinning of the perpendicular driven string shown in Fig. 1. The transversely driven parallel moving string does not become more disordered as observed at the depinning transition of the strictly perpendicular driven string. Instead, the transverse depinning occurs through the formation of a running kink that moves in the direction of the longitudinal drive as seen in Fig. 5. Although one might expect a kink and an anti-kink to form, we observed that below the kink the string is positioned at a slight angle. The kink moves along the string through the periodic boundary conditions. As the transverse drive is increased more kinks appear and the kinks begin to move more rapidly. Similar kink motion has been observed in interfaces in sliding friction systems [27]. The moving kinks themselves can show intricate dynamics. We have observed that these kinks can become pinned, and that another kink can form elsewhere and later collide with the pinned kink to form a larger kink.

In conclusion we have numerically investigated the dynamics of perpendicular and parallel driven strings in

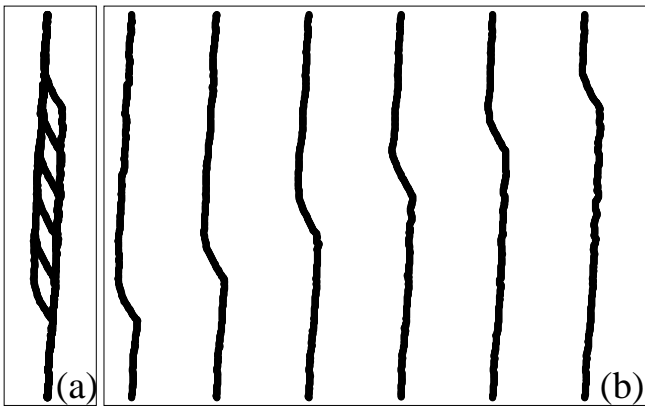


FIG. 5. (a) A series of snapshots of a parallel driven string as a function of time with the longitudinal drive in the y -direction and the transverse drive in the x -direction, for a system with $F_d = 0.12$, just above the transverse depinning threshold. The transverse depinning occurs via formation of a running kink that moves in the direction of the longitudinal drive. (b) The same snapshots offset in the x direction.

quenched disorder. We find that the string is most disordered at the depinning transition but recovers order for increasing drive as measured by the difference between the length of the string and the equilibrium length. This reordering is observable in the noise characteristic. Broad $1/f^2$ noise is observed at depinning, with a gradual reduction in the noise power for increasing drive and a shift to a whiter noise characteristic. For the parallel driven moving string we find that there is a finite transverse critical depinning threshold F_{dp}^T , indicating that the theory of Ref. [11] regarding the transverse barrier in a very different system still appears to apply to this system. We see a decrease of F_{dp}^T with increasing longitudinal drive, as predicted in Ref. [18] for CDW's, and find that the decrease follows a power-law form as predicted [26]. The transverse depinning occurs by the formation of longitudinal kinks. We do not observe a transverse depinning threshold for the perpendicular driven string. Possible experimental systems in which to investigate the predications in this work include noise measurements and domain wall imaging for magnetic domains driven at increasing magnetic field sweep rates, as well as varied moving contact line speeds over a rough surface for increased drive. Our prediction for the reordering and the transverse barrier for the parallel driven string may be observable in polymers aligned with the drive in disordered media or a single stream of liquid flowing over a rough surface at various longitudinal and transverse tilt angles.

We thank M. Chertkov, T. Germann, L. Radzihovsky, and G. Zimányi for useful discussions. This work was supported by the US Department of Energy under contract W-7405-ENG-36.

[1] G. Bertotti, *Hysteresis in Magnetism* (Academic Press, 1998).

- [2] A.-L. Barabasi and H.E. Stanley, *Fractal Concepts in Surface Growth* (Cambridge University Press, Cambridge, 1995); T. Halpin-Healy and Y.C. Zhang, Phys. Rep. **254**, 214 (1995).
- [3] T. Kawaguchi and H. Matsukawa, Phys. Rev. B **61**, R16366 (2000).
- [4] G. Blatter *et al.*, Rev. Mod. Phys. **66**, 1125 (1994).
- [5] L. Sneddon, M.C. Cross, and D.S. Fisher, Phys. Rev. Lett. **49**, 292 (1982); G. Gruner, Rev. Mod. Phys. **60**, 1129 (1988); L. Balents and M.P.A. Fisher, Phys. Rev. Lett. **75**, 4270 (1995); L.W. Chen, L. Balents, M.P.A. Fisher, and M.C. Marchetti, Phys. Rev. B **54**, 12 798 (1996).
- [6] S. Bhattacharya and M.J. Higgins, Phys. Rev. Lett. **70**, 2617 (1993).
- [7] U. Yaron *et al.*, Nature (London) **376**, 753 (1995); M.C. Hellerqvist *et al.*, Phys. Rev. Lett. **77**, 4022 (1996); W. Henderson *et al.*, Phys. Rev. B **77**, 2077 (1996); F. Pardo *et al.*, Phys. Rev. Lett. **78**, 4633 (1997).
- [8] F. Pardo *et al.*, Nature (London) **396**, 348 (1998).
- [9] A.M. Troyanovski, J. Aarts, and P.H. Kes, Nature (London) **399**, 665 (1999).
- [10] A.E. Koshelev and V.M. Vinokur, Phys. Rev. Lett. **73**, 3580 (1994).
- [11] T. Giamarchi and P. Le Doussal, Phys. Rev. Lett. **76**, 3408 (1996); **78**, 752 (1997); P. Le Doussal and T. Giamarchi, Phys. Rev. B **57**, 11356 (1998).
- [12] L. Balents, M.C. Marchetti, and L. Radzihovsky, Phys. Rev. Lett. **78**, 751 (1997); Phys. Rev. B **57**, 7705 (1998).
- [13] S. Scheidl and V.M. Vinokur, Phys. Rev. E **57**, 2574 (1998).
- [14] K. Moon, R.T. Scalettar, and G.T. Zimányi, Phys. Rev. Lett. **77**, 2778 (1996); S. Ryu *et al.*, Phys. Rev. Lett. **77**, 5114 (1996).
- [15] N. Grønbech-Jensen, A.R. Bishop, and D. Dominguez, Phys. Rev. Lett. **76**, 2985 (1996); M.C. Faleski, M.C. Marchetti, and A.A. Middleton, Phys. Rev. B **54**, 12 427 (1996); S. Spencer and H.J. Jensen, *ibid.* **55**, 8473 (1997); A.B. Kolton, D. Dominguez, and N. Grønbech-Jensen, Phys. Rev. Lett. **83**, 3061 (1999).
- [16] C.J. Olson, C. Reichhardt, and F. Nori, Phys. Rev. Lett. **81**, 3757 (1998).
- [17] C.J. Olson and C. Reichhardt, Phys. Rev. B **61**, R3811 (2000).
- [18] L. Radzihovsky and J. Toner, Phys. Rev. Lett. **17**, 3711 (1998).
- [19] N. Markovic *et al.*, Phys. Rev. Lett. **84**, 534 (2000).
- [20] M. Dong, M.C. Marchetti, A.A. Middleton, and V.M. Vinokur, Phys. Rev. Lett. **70**, 662 (1993).
- [21] H. Kaper, G. Leaf, D. Levine, and V.M. Vinokur, Phys. Rev. Lett. **71**, 3713 (1993).
- [22] H. Leschhorn and L.-H. Tang, Phys. Rev. Lett. **70**, 2973 (1993).
- [23] H. Makse, A.L. Barabasi, and H.E. Stanley, Phys. Rev. E **53**, 6573 (1996).
- [24] D.S. Fisher, Phys. Rev. Lett. **50**, 1486 (1983).
- [25] A.C. Marley, M.J. Higgins, and S. Bhattacharya, Phys. Rev. Lett. **74**, 3029 (1995).
- [26] L. Radzihovsky, private communication.
- [27] T.C. Germann, private communication.